



Redefining the Koizumi model of mouse cerebral ischemia: A comparative longitudinal study of cerebral and retinal ischemia in the Koizumi and Longa middle cerebral artery occlusion models

Helena Justić^{1,2,*}, Anja Barić^{1,2,*}, Iva Šimunić² ,
Marin Radmilović³ , Rok Ister^{1,2}, Siniša Škokić¹  and
Marina Dobrivojević Radmilović^{1,2} 

Abstract

Cerebral and retinal ischemia share similar pathogenesis and epidemiology, each carrying both acute and prolonged risk of the other and often co-occurring. The most used preclinical stroke models, the Koizumi and Longa middle cerebral artery occlusion (MCAO) methods, have reported retinal damage with great variability, leaving the disruption of retinal blood supply via MCAO poorly investigated, even providing conflicting assumptions on the origin of the ophthalmic artery in rodents. The aim of our study was to use longitudinal *in vivo* magnetic resonance assessment of cerebral and retinal vascular perfusion after the ischemic injury to clarify whether and how the Koizumi and Longa methods induce retinal ischemia and how they differ in terms of cerebral and retinal lesion evolution. We provided anatomical evidence of the origin of the ophthalmic artery in mice from the pterygopalatine artery. Following the Koizumi surgery, retinal responses to ischemia overlapped with those in the brain, resulting in permanent damage. In contrast, the Longa method produced only extensive cerebral lesions, with greater tissue loss than in the Koizumi method. Additionally, our data suggests the Koizumi method should be redefined as a model of ischemia with chronic hypoperfusion rather than of ischemia and reperfusion.

Keywords

Brain, ischemia, magnetic resonance angiography, mice, retina

Received 2 January 2022; Revised 24 April 2022; Accepted 27 May 2022

Introduction

Approximately 65% of ischemic stroke incidents are accompanied by temporary or permanent visual field loss, contributing to stroke-induced disability burden.^{1,2} Although stroke-related visual field loss usually occurs due to the involvement of the optic radiation or visual cortex, patients with stroke also have a higher risk of acute retinal ischemia and vice versa.^{3–6} This reflects the fact that retina develops from the diencephalon and, as such, shares anatomical and functional characteristics with the brain, including the blood supply through the internal carotid artery (ICA).⁷ Since retinal changes can be directly visualized and monitored longitudinally in a non-invasive manner,

studying the co-occurring retinal ischemia could lead to a better understanding of stroke.

¹Croatian Institute for Brain Research, University of Zagreb School of Medicine, Zagreb, Croatia

²Department of Histology and Embryology, University of Zagreb School of Medicine, Zagreb, Croatia

³Department of Ophthalmology, Sestre Milosrdnice University Hospital Center, Zagreb, Croatia

*These authors contributed equally to this work.

Corresponding author:

Marina Dobrivojević Radmilović, University of Zagreb School of Medicine, Šalata 3, 10000 Zagreb, Croatia.
Email: marina.radmilovic@mef.hr

In rodents, stroke is often modeled by transient occlusion of the middle cerebral artery (MCA), mimicking the majority of human ischemic lesions occupying the MCA territory.⁸ In the filament MCA occlusion (MCAO) model, a filament is introduced into the common carotid artery (CCA) toward the ICA (the Koizumi model) or from the external carotid artery (ECA) into the ICA (the Longa model), and advanced to the origin of the MCA, resulting in a reduction of perfusion with subsequent infarction of subcortical, as well as primary motor and sensory cortical regions.^{9,10} In the setting of these methods, transient or permanent CCA and ECA ligation and transient occlusion of the branches of the ICA by the filament also interrupts or reduces the vascular supply to the retina. Studies of retinal ischemia in different MCAO models commonly reported either electroretinographic, perfusion, or gene expression changes, but evidence of morphological damage was inconsistent.^{11–15} The varying outcomes may have been affected by differences in MCAO duration, different approaches resulting in permanent ECA or CCA ligation, modifications including contralateral CCA or ipsilateral pterygopalatine artery (PPA) ligation, intraluminal filament length, non-uniform distribution of ischemic lesions, choice of outcome assessment, etc. Studies outside of the MCAO scope, such as those modeling chronic cerebral and retinal hypoperfusion, showed similarly conflicting results.^{16–20} Additionally, species and strain-related differences in vascular anatomy and reactivity may influence cerebral and retinal susceptibility to ischemic damage in different experimental procedures.²¹ In fact, a number of MCAO studies mistakenly depict murine vascular anatomy as identical to human, where the ophthalmic artery (OA) originates from the ICA just proximally to the origin of the MCA,^{12,14} and not from the PPA as has been documented in rats²² and seems to be the case in mice.^{23,24}

Unfortunately, even though previous studies analyzed retinal changes in different models of acute or chronic cerebral or retinal ischemia, none of them provided anatomical evidence of the origin of the ophthalmic artery in the experimental animals. Additionally, regardless of their interest in co-occurring retinal ischemia, none of the MCAO studies to date quantified the long-term status of either cerebral or retinal vascular perfusion after MCAO. Since these basic questions had been poorly addressed, in this study we aimed to use the advantages of longitudinal *in vivo* magnetic resonance imaging (MRI) to clarify if and how the two most used modifications of the MCAO method induce retinal ischemia, how they affect cerebral and retinal perfusion both acutely and in the long term, how they differ in regard to the evolution of the ischemic lesion, and how these differences reflect on the

possibility of using the accessibility of the retina to study the brain.

Materials and methods

All animal handling and procedures were approved by the Ethics Licensing Committee of the University of Zagreb School of Medicine and the Ethics Committee for the protection of animals used for scientific purposes of the Ministry of Agriculture of the Republic of Croatia. Experimental procedures were conducted according to Croatian Animal Protection Act (NN 102/17, 32/19), Amendments to the Animal Protection Act (NN 37/13) and the Guidelines on the Protection of Animals Used for Scientific Purposes (NN 55/13) which are in line with the European Guide for the Care and Use of Laboratory Animals (Directive 2010/63/EU). All reported experiments followed the ARRIVE guidelines. The experiments were carried out on 33 male C57Bl/6J mice, 3–6 months old, bred at the animal facility of the Croatian Institute for Brain Research, University of Zagreb School of Medicine. The animals were housed on a 12-hour light-dark cycle in a humidity-controlled environment at $22 \pm 2^\circ\text{C}$. Water and pelleted food were given *ad libitum*.

Sample calculation

Based on our preliminary data, a power analysis performed with G*Power software²⁵ (power = 0.8; alpha = 0.05; two-sided Mann-Whitney U-test) estimated 7 animals per MCAO group would be required to detect differences in lesion volume. However, to account for attrition due to expected mortality rate of up to 30%, sample size was corrected to 10 animals per each MCAO group ($N_{\text{corrected}} = N / (1 - [\% \text{ attrition} / 100])$). The number in the Koizumi-sham group was corrected to 8 (10% attrition) and reduced to 5 in the Longa-sham group (preliminary data showed no changes in retina or brain in this group).

Middle cerebral artery occlusion (MCAO) method

Cerebral ischemia was induced by a 30-minute occlusion of the left MCA using the Koizumi (CCA-MCAO) or Longa (ECA-MCAO) intraluminal filament method.^{9,10} Preoperatively, the mice were injected with 0.25 ml of buprenorphine (0.05 mg/kg Buprenovet, Bayer, Germany) and 0.5 ml of saline with 20% glucose intraperitoneally (i.p.) to relieve pain and prevent dehydration. Anesthesia was induced with 4% isoflurane (Isofluran-Piramal, Piramal Critical Care, Germany) and maintained with 1.5–2% isoflurane. Body temperature was monitored and maintained at $37^\circ\text{C} \pm 0.5^\circ\text{C}$ using a temperature-controlled

heating pad and a rectal temperature probe. To prevent corneal drying the eyes were covered with ophthalmic ointment (Recugel, Bausch and Lomb, Canada). The temporal region was shaved, disinfected, and an incision was made to place a calibrated 1 mm diameter laser probe against the temporal bone to monitor the blood flow changes of the distal portion of the MCA on a laser-Doppler perfusion monitor (moorVMS-LDF1, Moor Instruments, UK). After recording the perfusion value, the animals were placed in a supine position and the surgical field was shaved and disinfected. A midline neck incision was made between the manubrium of the sternum and the jaw exposing the left CCA, ICA, and ECA. For the Koizumi method ($n = 10$), after permanent ligation of the CCA, a monofilament (7019910-6021910, Doccol Corporation, USA) was introduced through an incision in the CCA and advanced through the circle of Willis up to the MCA. For the Longa method ($n = 10$), after ligation (transient) of the CCA and permanent ligation of the ECA, a monofilament was introduced through an incision in the ECA and advanced to the MCA. In both MCAO groups, after a 30-minute occlusion period, animals were re-anesthetized and the monofilament was withdrawn. Sham surgeries were performed for both methods by inserting the monofilament and immediately withdrawing it ($n = 8$ for CCA sham; $n = 5$ for ECA sham). Block randomization (day of experiment) was used for group allocation. For three days post-surgery mice received i.p. injections of 250 μ l saline to prevent dehydration and buprenorphine (0.05 mg/kg, 0.25 ml) to achieve analgesia.

Neurological deficit scoring and weight loss measurement

Scoring of neurological deficits (NDS) and weight measurements were performed 7 days prior to and 2, 9, and 35 days after MCAO. The NDS was performed as a sequence of different tests assessing motor (muscle status, gait disturbance, and spontaneous activity) and sensory (tactile and proprioceptive) status, the functionality of reflexes, and appearance, on a scale of 0–39.^{10,26,27} Higher scores indicated greater severity of the injury. Weight loss was compared to baseline pre MCAO weight and scored as follows: no weight loss = 0 points, less than 5% = 1 point, 5%–15% = 2 points, 15%–20% = 3 points.

Magnetic resonance imaging

MRI experiments were carried out on a 7 T system (BioSpec 70/20 USR with Paravision 6.0.1. software version, Bruker Biospin, Germany) in a Tx/Rx configuration, using an 86 mm transmit volume coil and a 2-

element mouse brain surface receive coil (MT0381, MT0042, Bruker Biospin, Germany). Anesthesia was induced with 4% isoflurane (Isofluran-Piramal, Piramal Critical Care, Germany) in a 30/70% O₂/N₂ mixture and maintained with 1.5–2% isoflurane during scanning. Respiratory rate was monitored with an optical probe (Medres, Germany) and maintained at 80–100 breaths per min. The body temperature was monitored using an MR-compatible rectal temperature probe (Medres, Germany) and maintained at $37 \pm 0.5^\circ\text{C}$ via a feedback-controlled circulating heating pump. Animals were imaged 7 days before MCAO to assess the baseline state and 2, 9, and 35 days after MCAO. T2-weighted images of the brain were acquired in the coronal plane using a RARE sequence with time of echo/time of repetition (TE/TR = 33/3000 ms; matrix size 160×100 ; field of view (FOV) $16 \times 10 \text{ mm}^2$; slice thickness 0.4 mm; interslice distance 0.1 mm; number of slices 25. T2-maps of the brain were obtained using an MSME sequence with TE/TR = 7.5/3150 ms; matrix size 128×80 ; FOV $16 \times 10 \text{ mm}^2$; slice thickness 0.4 mm; interslice distance 0.1 mm; number of slices 25. Values were calculated from measured data using Paravision 6.0.1. software (Bruker Biospin, Germany) built-in post-processing macros. Gradient-echo images for whole-brain angiographies were acquired using a 3D FLASH sequence (3D-TOF) with TE/TR = 2.1/12.0 ms, flip angle 25° , matrix size $200 \times 150 \times 70$, FOV $16 \times 12 \times 14 \text{ mm}^3$. T2-weighted images of the eyes were acquired using a RARE sequence with TE/TR = 28/2500 ms; matrix size 166×100 ; FOV $10 \times 6 \text{ mm}^2$; slice thickness 0.4 mm; interslice distance 0.1 mm; number of slices 9, with the central slice bisecting the center of the eye and the optic nerve sagittally, minimizing the partial-volume effect due to the curvature of the retina. Total duration of the imaging session was approximately 60 minutes per mouse.

MRI exclusion criteria were applied after the first post-MCAO imaging session and consisted of an indiscernible lesion or lesion volume below 20 mm^3 , which was considered strongly suggestive of surgical error.

MRI data processing

MR images of the brains and eyes were analyzed semi-automatically using ImageJ 1.53i software (Wayne Rasband, National Institutes of Health, USA) by experienced investigators blind to the experimental groups.

Volumetric analysis of the brain

Lesion volume was assessed on the T2-map images by delineation of the hyperintense area under vasogenic edema. Ventricle volume was measured from T2-map

images via a semi-automatic procedure using an in-house developed macro for FIJI/ImageJ v.1.53c. The macro automatically detects all points inside the brain hemisphere ROI with a measured T2 value higher than the highest T2 value of healthy tissue ($T2 > 65$ ms). The measured lesion volume was subtracted from the hemisphere ROI before the automatic detection step. Hemisphere volumes were analyzed on T2-weighted images using a standardized semi-manual segmentation pipeline after deducing the volume of the ventricles. Hemisphere swelling in the acute phase or tissue atrophy in the chronic phase were expressed as a percent increase of the hemisphere volume in respect to the hemisphere volume at baseline. Tissue loss was expressed as a difference between the ipsilateral hemisphere volume at baseline and the ipsilateral hemisphere volume at the time point measured.

Retinal thickness analysis

Retinal thickness was assessed using a single T2-weighted mid-sagittal slice bisecting the center of the eye and the optic nerve, measuring in 3 points superiorly and 3 inferiorly from the optic nerve head. Segmentation was performed at sub-pixel accuracy on linearly interpolated subsampled T2-weighted images, smoothed by Anisotropic Diffusion 2D filter. The measuring positions were determined after defining the center of the eyeball and drawing radial projections perpendicular to the retina.

Angiographic analysis

Angiograms were obtained from 3D-TOF-scans by generating maximum intensity projections (MIP) using Paravision6.0.1.-software enabling visualization and inspection of vasculature with high blood flow velocity. The vessel volume for each hemisphere was analyzed in a cuboid 3D-ROI occupying the ventral half of the 3D-FOV, measuring the volume of major arteries of the brain and neck. The volume and the position of the ROI were standardized using anatomical landmarks at the anterior, posterior, and superior parts of the ROI. The extracted ROI was used for further analysis. The segmentation was performed using the open-source machine learning plugin in FIJI/ImageJ-v.1.53c to create an optimized script to get vessel volume and density parameters. After thresholding and binarization, volumetric analysis was performed on the obtained final image of the objects and expressed as vessel volume of the ipsilateral/contralateral hemisphere in mm^3 . A manual quantitative assessment of the posterior communicating artery (PcomA) recruitment was performed based on previously described methods.^{28,29}

Histological and immunohistochemical analysis

After the last MRI session 35 days after MCAO, the animals were anesthetized with an intraperitoneal injection of 2.5% tribromoethanol (Avertin, Sigma Aldrich, USA), transcardially perfused with 30 ml of phosphate-buffered saline (PBS), followed by 30 ml of PBS-buffered 4% paraformaldehyde (Sigma Aldrich, USA). The eyes were enucleated and postfixed for 24 hours in Davidson's solution at room temperature, then transferred to 10% neutral buffered formalin overnight. Eyes were then dehydrated in increasing concentrations of ethanol (70% and 96% two times for 1.5 hours, then 100% ethanol (Biognost, Croatia) overnight, followed by a mixture of 100% ethanol/Bioclear xylene (Biognost, Croatia) 1:1 for 1.5 hours and Bioclear xylene twice for 1.5 hours), then permeated three times in paraffin (Sakura, Japan) at 60°C for 2 hours, and embedded in paraffin (Histoplast Thermo Scientific, UK). The eyes were cut into 6 μm sections on a rotary microtome.

For histological and immunohistochemical analysis, sections in the mid-sagittal area were deparaffinized with Bioclear xylene twice for 5 min, then rehydrated in a series of baths with decreasing ethanol concentration (100% twice for 5 minutes, 96% for 2 minutes, and 70% for 2 minutes). For the histological examination, slices were rinsed twice in distilled water for 1 minute, stained with Mayer's Hematoxylin (Merck, Germany) for 5 minutes, rinsed twice in water for 1 minute, stained with Eosin (Merck, Germany), then rinsed twice in water and dehydrated in a series of baths with increasing ethanol concentration (70%, 96% twice, and 100% twice for 20 seconds). To lighten the sections, Bioclear xylene was applied twice for 1 minute, after which slides were coverslipped with Biomount mounting media (Biognost, Croatia), dried overnight and examined using a light microscope (Olympus BX53F2, USA).

For immunohistochemical analysis, after rehydration the sections were rinsed 4 times in PBS, followed by antigen retrieval in Tris-HCl-EDTA-SDS (250 mM tris(hydroxymethyl)aminomethane (Kemika, Croatia), 10 mM ethylenediaminetetraacetate (Kemika, Croatia) and 0.5% (w/v) sodium dodecyl sulfate), at pH 8.5, 4 times for 10 minutes at 95°C. After cooling, the sections were washed with PBS, then blocked using PBS with 0.25% Triton-X-100 (Sigma-Aldrich, USA) and 10% goat serum (Gibco, USA). The primary antibody mouse anti-neuronal nuclei (NeuN; 1:200; MAB377, Millipore, USA), was diluted in PBS with 0.1% Triton-X-100 and 1% goat serum and applied overnight at room temperature. The secondary antibody Alexa Fluor 488 goat anti-mouse (1:500; A11001,

Invitrogen, USA), was applied for 2 hours at room temperature. The cell nuclei were stained using 4'6-diamidino-2-phenylindole (DAPI 1 mg/ml, Thermo Fisher Scientific, USA). Stained sections were mounted with fluorescent mounting medium (DAKO, USA) and examined using a confocal fluorescence microscope (Olympus FV3000, USA).

Images were analyzed using ImageJ 1.53i software. Retinal thickness was assessed in 4 animals per group, measuring in 4 points laterally from the optic nerve head. The measuring positions were determined after defining the center of the eyeball and drawing radial projections perpendicular to the retina. To quantify the number of ganglion cells expressing NeuN, three regions of interest (ROI size 100 μ m) per image were used. Four images per ROI were taken. The neuronal nuclei marker expressing cells were manually counted in 4 animals per group.

Statistical analysis

Statistical analysis was performed using Graph Pad Prism (GraphPad Software, USA). The survival analysis was performed by calculating survival proportions using the product limit Kaplan-Meier method. After confirming normal distribution using the Shapiro-Wilk test, a mixed model two-way analysis of variance (ANOVA) with time and surgery as factors was used to evaluate weight, MCA perfusion, neurological status, normalized ipsilateral and contralateral hemisphere volume, swelling and tissue atrophy, tissue loss, and retinal thickness. Post hoc comparisons were performed using Tukey's multiple comparisons test. For ischemic lesion volume and immunohistochemical analysis evaluation two-way ANOVA with Sidak post hoc comparisons test was performed. Statistical significance was defined as $P < 0.05$. Data were presented as

mean values \pm standard deviation or median with inter-quartile range.

Results

Survival and weight

From 20 animals which underwent MCAO surgery, one animal from the CCA-MCAO group was excluded from the study after the first imaging session due to a lacunar lesion outside of the MCA territory. Since hemorrhagic transformation occurs after reperfusion in approximately 25% of ECA-MCAO cases,³⁰ one animal from the ECA-MCAO group which developed a hemorrhagic transformation after the first imaging session was kept in the analysis. The lesion size measured without the hemorrhage volume was equal to the average lesion volume of the group. For both MCAO modifications, most deaths ($n = 4$) occurred within the first week after MCAO.

The survival analysis showed no significant difference in survival curves between groups (Log-rank (Mantel-Cox) test; $P = 0.0616$), however, there was a difference in trend (Log-rank test for trend; $P = 0.0242$) which arose from the survival proportions after the first week, where 88.9% of animals undergoing the CCA-MCAO survived, compared to 66.9% survival for the ECA-MCAO group (Figure 1(a)).

All groups showed weight loss in the first 48 hours (Figure 1(b)). The CCA-MCAO group and sham groups regained weight toward day 9 in contrast to the ECA-MCAO group, which still had significantly lower bodyweight ($P < 0.0001$). The MCAO groups regained baseline bodyweight towards the last time point, in contrast to the sham groups which gained additional weight ($P < 0.0001$; Figure 1(b)).

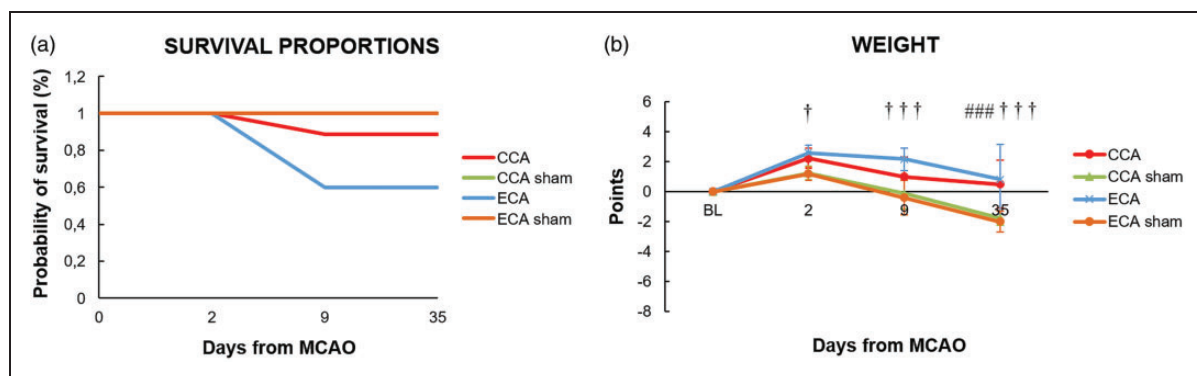


Figure 1. Survival proportions and animal weight after middle cerebral artery occlusion by filament insertion through the common carotid artery (CCA), external carotid artery (ECA), and the ECA or CCA sham-operated (CCA sham and ECA sham) animals. Statistical differences using a mixed model ANOVA and Tukey post hoc test for ECA to ECA sham group (†) $P < 0.05$; (†††) $P < 0.001$; CCA to CCA sham group (####) $P < 0.001$. Error bars represent standard deviation.

Laser Doppler flowmetry analysis shows incomplete reperfusion of the MCA in the CCA method

To assess the perfusion status of the MCA, laser-Doppler flowmetry (LDF) was performed during surgery. The LDF signal significantly decreased after filament insertion for both MCAO groups (baseline vs. occlusion, $P < 0.0001$; Figure 2). Due to permanent ligation of the CCA, the CCA-sham group also showed a significant decrease in LDF signal ($P < 0.0001$). After filament withdrawal, the LDF signal showed complete reperfusion only in the ECA-MCAO group. In the CCA-MCAO group the reperfusion was incomplete compared to both ECA-MCAO group ($P < 0.0001$) or CCA-sham ($P < 0.0001$), pointing to the hypoperfusion status of the MCA territory in this surgical model (Figure 2).

High-resolution MR angiography uncovers chronic ipsilateral hypoperfusion in the CCA method

To assess the vascular perfusion, high-resolution MR angiography (MRA) was performed. The baseline 3D MIP reconstruction clearly showed that in all our C57Bl6J mice the PPA (green arrow) gave rise to the OA (yellow arrow; Figure 3(a,BL) and Supplementary Figure 3). It also showed striking variability of the vasculature, from tortuous stair-like ICA, S-shaped distal portion of the ICA, to looping of the PCA narrowing the diameter of the circle of Willis (Supplementary Figure 1). Two days after MCAO, the MIP of the

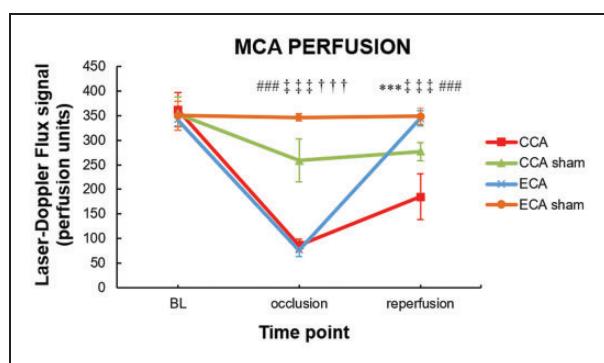


Figure 2. Intraoperative laser Doppler flowmetry shows incomplete reperfusion in the Koizumi (CCA) middle cerebral artery occlusion method. Middle cerebral artery (MCA) perfusion measured with laser Doppler flowmetry during MCA occlusion (MCAO) by filament insertion through the common carotid artery (CCA), the external carotid artery (ECA), and sham surgeries (CCA sham and ECA sham). Statistical differences using mixed model ANOVA and Tukey post hoc test for the CCA to ECA group (***) $P < 0.001$; CCA to CCA sham group (###) $P < 0.001$; ECA to ECA sham group (†††) $P < 0.001$; CCA sham to ECA sham group (‡‡‡) $P < 0.001$. Error bars represent standard deviation.

ECA-MCAO group revealed lower signal intensity of the MCA (blue arrow; Figure 3(a,BL)), with a hypoperfused segment between the ipsilateral (IL) anterior cerebral artery (ACA) and MCA, and with no changes in the perfusion of the PPA or OA. The blood flow in the IL MCA of the ECA-MCAO group on day 9 regained baseline values. On day 35, the baseline levels of perfusion in the ECA-MCAO group were reestablished; however, the MIP showed path alteration with looping and kinking of the distal portion of the MCA (Figure 3(a,D35)). There was no recruitment of the IL PcomA in the measured time points (Supplementary Figure 4). The MIP and arterial volume measurements of the ECA-MCAO contralateral (CL) hemisphere (CLH), as well as those of the ECA-sham group, did not show significant changes. On day 2 after MCAO, the MIP analysis of the CCA-MCAO group showed hypoperfusion of the entire ILH with significant drop in arterial volume ($P < 0.0001$). There was no change in signal intensity of the CLH (Figure 3(a,D2)). On day 9 after MCAO, the perfusion of the ILH in the CCA-MCAO group was partially reestablished in the circle of Willis, posterior cerebral artery (PCA), proximal MCA, and ACA; however, the arterial volume was still significantly lower compared to baseline ($P = 0.0007$). Furthermore, attenuation of the blood flow persisted in the IL ICA, distal portion of the MCA, PPA, OA and segment between ACA and MCA, with prominent hyperperfusion of the CL ICA and segments between PCA and MCA, and MCA and ACA (Figure 3(a,D9)). On day 35, only the IL PPA, OA, and ICA still had undetectable signal intensity. The measured arterial volume did not reach baseline values at the last measured time point ($P = 0.0007$). Recruitment of the IL PcomA was detected in 5/9 animals (Supplementary Figure 4). The 3D MIP reconstructions revealed aberrant morphology of the circle of Willis and alterations in the entire path of the IL MCA, which became highly tortuous. The CCA-sham group showed hypoperfusion of the entire ILH with lower arterial volume compared to baseline ($P = 0.0008$) 2 days after sham surgery. The ILH signal normalized in the chronic phase, reaching baseline arterial volume values toward day 35. The CL ICA and the CL part of the circle of Willis showed acute and subacute signal intensity rise. The IL PPA and OA of the CCA-sham group had unidentifiable signal intensity at all measured time points.

MRI analysis of brain ischemic lesion evolution shows prominent differences between the CCA and ECA MCAO method

All experimental groups were monitored using high-resolution MRI to define and compare the temporal

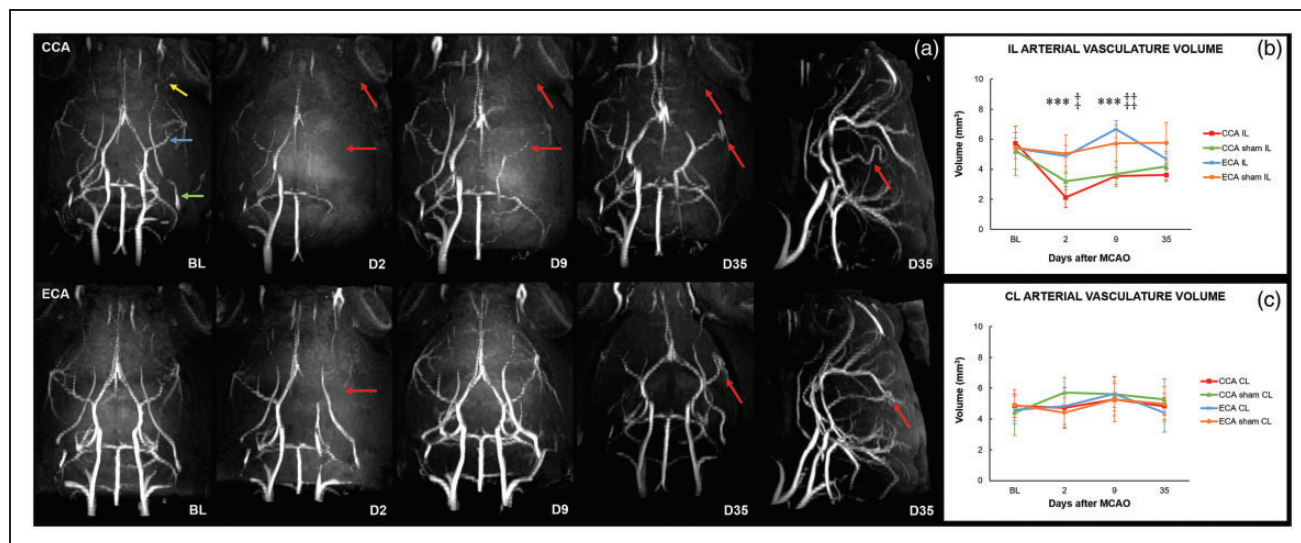


Figure 3. High-resolution MR angiography defines the Koizumi (CCA) middle cerebral artery occlusion method as a model of ischemia with chronic hypoperfusion. Maximum intensity projections (MIP) of MR angiography scans (a) and measured ipsilateral (b) and contralateral (c) arterial vasculature volume before and after middle cerebral artery occlusion (MCAO) by filament insertion through the common carotid artery (CCA; a-upper row) or external carotid artery (ECA; a-bottom row) show animals at baseline (BL) and on days 2 (D2), 9 (D9), and 35 (D35) after MCAO. Pre-surgery (BL) angiograms: yellow arrow – ophthalmic artery (OA); blue arrow – middle cerebral artery (MCA); green arrow – pterygopalatine artery (PPA). On D2, the MIP show hypoperfusion of the ipsilateral (IL) hemisphere in the CCA group. On D9, the attenuation of blood flow persists in the IL internal carotid artery (ICA), distal portion of the MCA, PPA, OA, and the segment between the anterior cerebral artery (ACA) and MCA, with prominent hyperperfusion of the contralateral (CL) ICA and the segments between the posterior cerebral artery (PCA) and MCA, and MCA and ACA. On D35, undetectable signal intensity of the IL PPA, OA, and ICA, with increased signal intensity of the CL ICA and the CL part of the circle of Willis. Tortuosity of the IL MCA (lateral view of CCA D35). On D2, the ECA-MCAO group shows lower signal intensity of the IL MCA with hypoperfused segment between the IL ACA and MCA, and no changes in the PPA or OA. On D9, the perfusion of the IL hemisphere is reestablished and slightly hyperperfused. On D35, the perfusion in the ECA-MCAO group shows baseline levels. Looping and kinking of the distal portion of the IL MCA (lateral view of ECA D35). Red arrows represent hypoperfused arteries or arterial tortuosity and path alteration. Statistical differences using mixed model ANOVA and Tukey post hoc test for the CCA to ECA group (***) $P < 0.001$; CCA sham to ECA sham group (‡) $P < 0.05$ (‡‡) $P < 0.01$. Error bars represent standard deviation.

profile of the ischemic lesion. T2-maps and T2-weighted image analysis at day 2 after MCAO revealed that both MCAO procedures induced the formation of large cortico-striatal lesions (Figure 4(a) and (e)). The ischemic lesion volume was significantly larger for the ECA-MCAO group compared to the CCA-MCAO group ($P = 0.0005$). The ischemic lesion volume in both MCAO groups decreased in size toward day 9. Both sham groups showed no change compared to baseline measurements.

To address the hemispheric changes induced by lesion and edema formation, the volumes of ILH and CLH were measured and compared between groups (Figure 4(b) and (d)). In both MCAO groups, the ILH volume significantly expanded from baseline to day 2 after MCAO ($P < 0.0001$), then shrank to and below baseline values at the beginning of the 2nd week (CCA-BL vs. D9 $P = ns$; ECA-BL vs. D9 $P = 0.0094$), after which it continued to significantly diminish in size toward day 35 ($P < 0.0001$). On day 2, the size of the ILH of the ECA-MCAO group was significantly

larger than in the CCA-MCAO group ($P < 0.0001$). On day 35, the ECA-MCAO group showed a more prominent ILH shrinkage compared to the CCA-MCAO group ($P = 0.0002$). In both MCAO groups, as the ILH enlarged on day 2 after MCAO, the CLH significantly contracted in size, compensating for the ILH expansion in a confined intracranial space (CCA-BL vs. D2 $P = 0.0165$; ECA-BL vs. D2, $P < 0.0001$).

To address both the edema formation in the acute phase and tissue atrophy in the chronic phase of ischemia, the ILH volume change was expressed as a percentage of baseline ILH volume and referred to as either swelling or tissue atrophy. Acutely, MCAO induced significant swelling of the ILH in both groups ($P < 0.0001$; Supplementary Figure 2). However, greater hemisphere swelling in the ECA-MCAO group on day 2 ($P < 0.0001$) induced significant tissue atrophy ($P < 0.0097$; Supplementary Figure 2) and tissue loss ($P = 0.0305$; Figure 4(c)) already on day 9 ($P < 0.0097$), which was further exacerbated in the chronic phase of ischemia. At 35 days after MCAO,

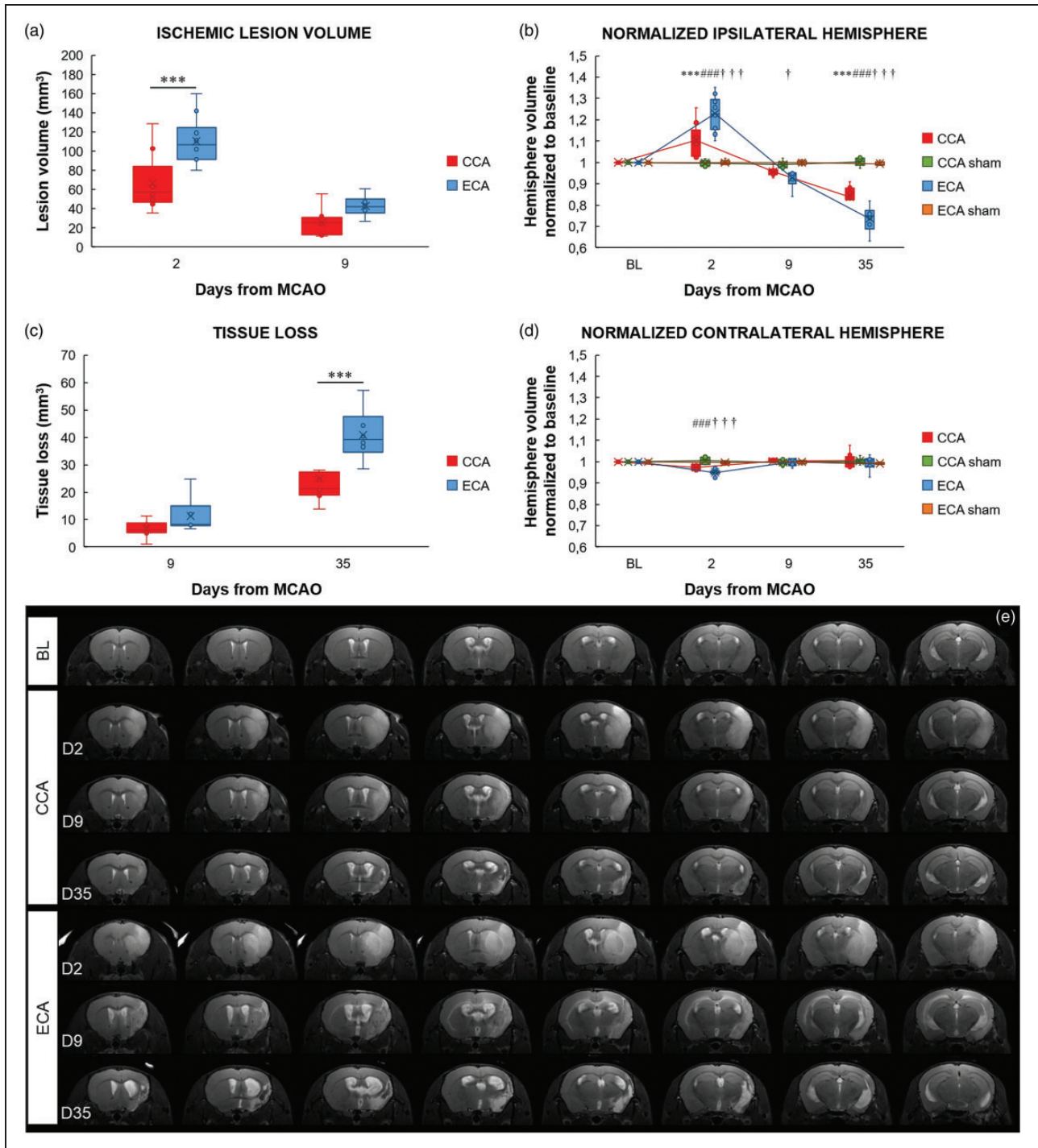


Figure 4. The Longa (ECA) middle cerebral artery occlusion method exacerbates the ischemic lesion and edema formation in the acute phase and tissue loss in the chronic phase. Ischemic lesion volume (a), normalized ipsilateral (b) and contralateral (d) hemisphere volume, and tissue loss (c) after middle cerebral artery occlusion (MCAO) by filament insertion through the common carotid artery (CCA), the external carotid artery (ECA), and in sham-operated (CCA sham and ECA sham) animals, measured before (baseline - BL) and on day 2 (D2), 9 (D9), and 35 (D35) after MCAO. Representative magnetic resonance T2 images of the mouse brain at baseline and after CCA or ECA MCAO at the measured time points (e). Statistical differences for the normalized ipsilateral and contralateral hemisphere volume and tissue loss using the mixed model ANOVA and Tukey post hoc test, and for the ischemic lesion volume mixed model ANOVA and Sidak post hoc test: CCA to ECA group (***) $P < 0.001$; CCA to CCA sham group: (###) $P < 0.001$; ECA to ECA sham group (†††) $P < 0.001$, (†) $P < 0.05$. Data presented as median with interquartile range.

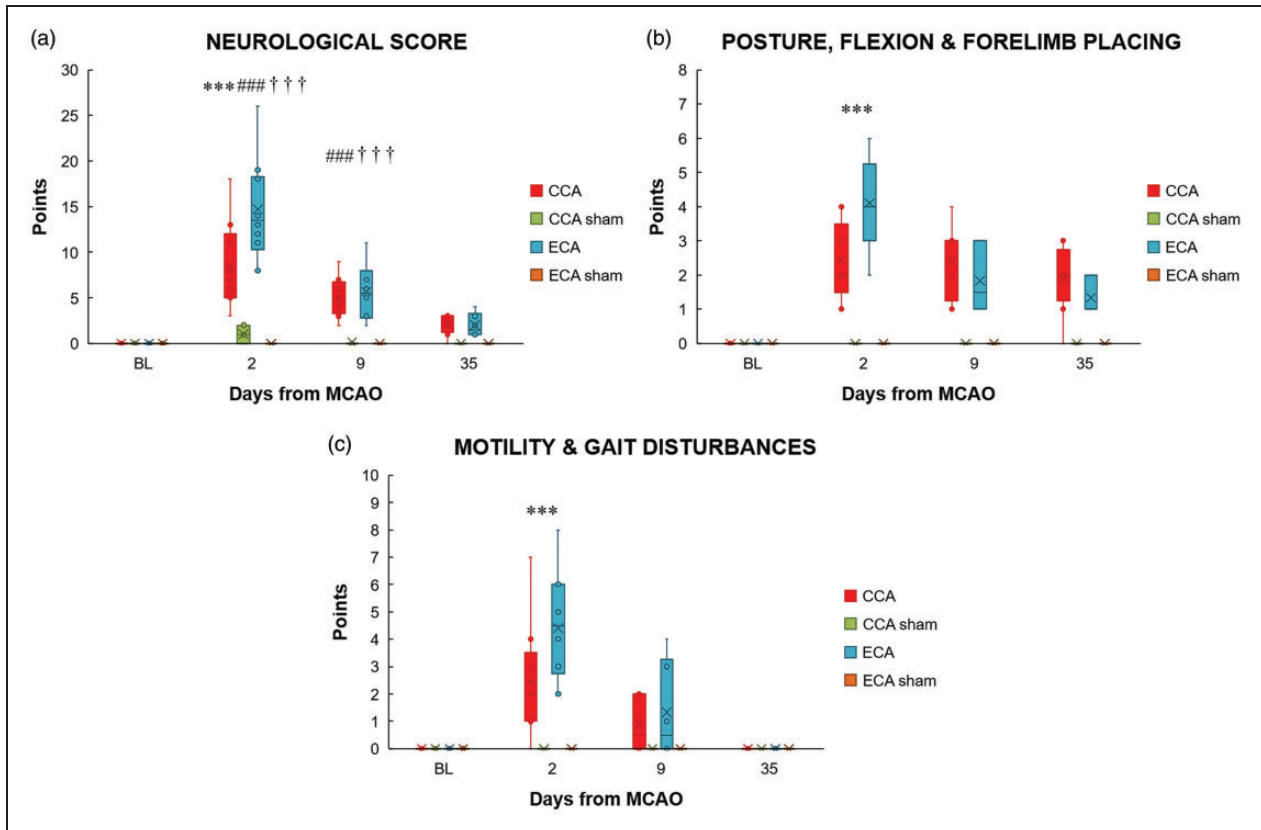


Figure 5. The Longa (ECA) middle cerebral artery occlusion method aggravates the neurological status in the acute phase of stroke. The neurological score (a), posture, flexion and forelimb placing (b), and motility and gait disturbances (c) before (baseline, BL) and 2 (D2), 9 (D9) and 35 (D35) days after middle cerebral artery occlusion (MCAO) by filament insertion through the common carotid artery (CCA), the external carotid artery (ECA), and in sham-operated (CCA sham and ECA sham) animals. Statistical differences using mixed model ANOVA and Tukey post hoc test for the CCA to ECA group (***) $P < 0.001$; CCA to CCA sham group (####) $P < 0.001$; ECA to ECA sham group (†††) $P < 0.001$. Data presented as median with interquartile range.

a highly significant tissue loss of the IL neocortex and striatum was present in both MCAO groups ($P < 0.0001$; Figure 4(c)), however to a lesser extent for the CCA-MCAO group.

In the ECA-MCAO method, in which full reperfusion follows the occlusion, significantly larger tissue swelling was observed, which further expanded the size of the ischemic lesion in the acute phase but also lead to greater tissue loss accompanied by ventriculomegaly and cyst formation in the chronic phase. By contrast, in the CCA-MCAO method, where chronic hypoperfusion followed the withdrawal of the filament, the acute tissue swelling and the chronic tissue loss, although severe, were less pronounced than in the ECA method (Figure 4(e)).

Functional outcome assessment shows poorer status in the acute phase for the ECA method

To assess the functional outcome after MCAO, neurological status was measured before each imaging

session. For both MCAO groups, the greatest deficit was on day 2. ($P < 0.0001$; Figure 5(a)). However, the ECA-MCAO group showed significantly poorer status compared to the CCA-MCAO group ($P < 0.0001$). Both MCAO groups regained neurological function toward day 35. When various parameters of the combined neurological score were separately analyzed, postural signs, motility and gait disturbances differed significantly between the MCAO groups in the acute phase ($P < 0.0001$; Figure 5(b) and (c)). In the chronic phase, although both groups regained baseline motility and gait, neither recovered to its baseline posture ($P < 0.0001$).

MRI analysis of retinal ischemic lesion evolution shows prominent differences between the CCA and ECA MCAO method

To address the impact of different surgical methods on retinal ischemic lesion evolution, the ipsilateral eye was monitored using high-resolution MRI for 35 days after

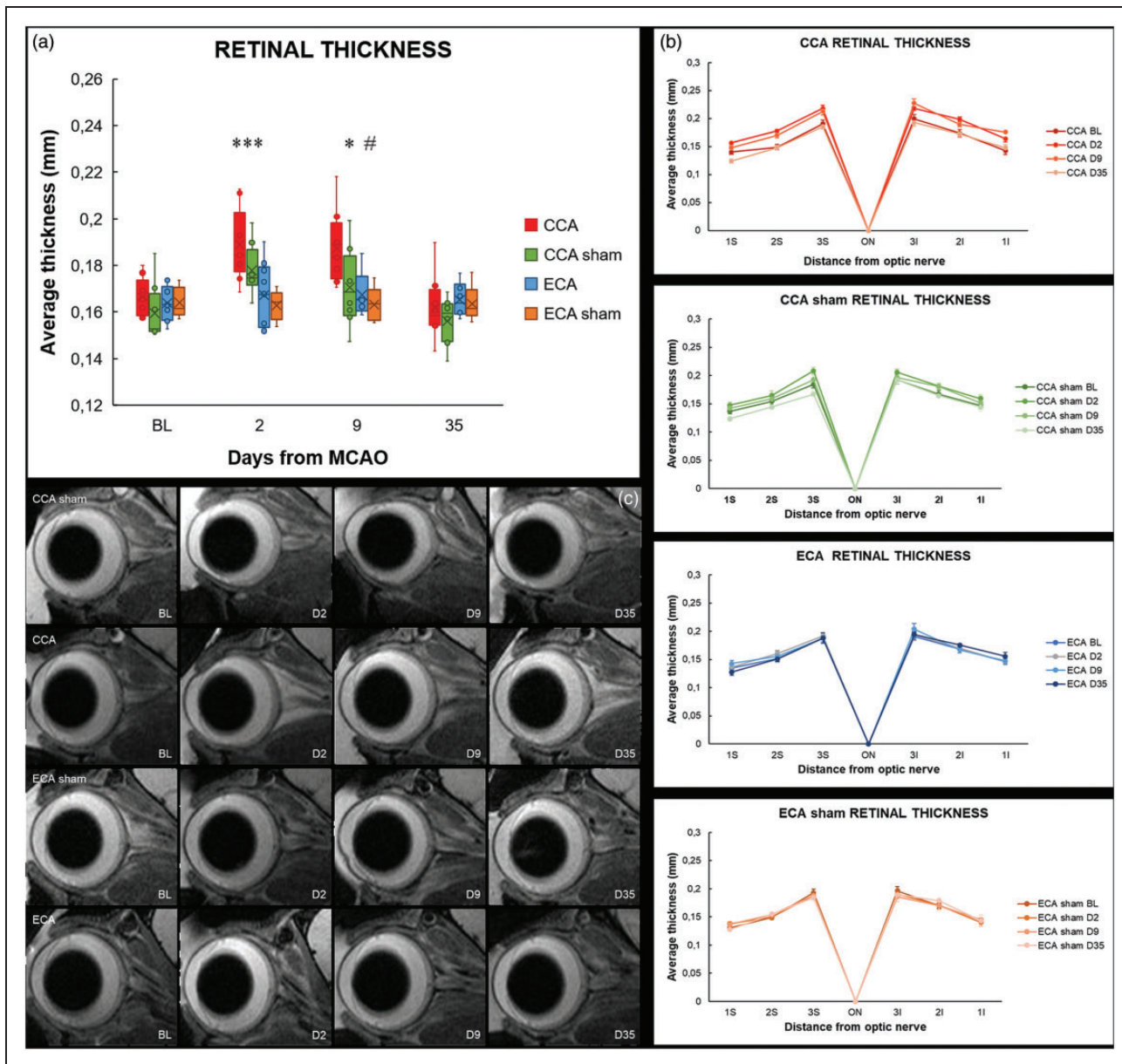


Figure 6. The Koizumi (CCA) middle cerebral artery occlusion method induces transient retinal thickening. The average retinal thickness (a), and retinal thickness in 3 points inferiorly and 3 superiorly from the optic nerve head (b) measured on a mid-sagittal T2-weighted anatomical magnetic resonance imaging scan bisecting the center of the eye and the optic nerve (c) after middle cerebral artery occlusion by filament insertion through the common carotid artery (CCA), the external carotid artery (ECA), and in sham-operated (CCA sham and ECA sham) animals. Statistical differences using mixed model ANOVA and Tukey post hoc test for the CCA to CCA sham group (***) $P < 0.001$, (*) $P < 0.05$; CCA to CCA sham group: (#) $P < 0.05$. Data presented as median with interquartile range.

MCAO. Two days after MCAO, there was a significant thickening of the retina in both CCA-MCAO and CCA-sham group compared to baseline (CCA-MCAO $P = 0.0006$; CCA-sham $P = 0.0098$). Interestingly, there was no change in retinal thickness in the ECA-MCAO nor the ECA-sham group (Figure 6 (a) and (b)). In the first week, the CCA-sham group regained baseline thickness values, in contrast to the CCA-MCAO group, in which the retina remained

significantly thicker when compared to baseline values ($P = 0.0024$; Figure 6(a) and (b)). The CCA-MCAO retinas regained their baseline thickness levels toward day 35. When comparing the MCAO groups, there was significant difference on days 2 and 9 after MCAO (D2 $P = 0.0008$; D9 $P = 0.0182$), indicating a distinct contrast of cerebral and retinal responses induced by the two different MCAO methods.

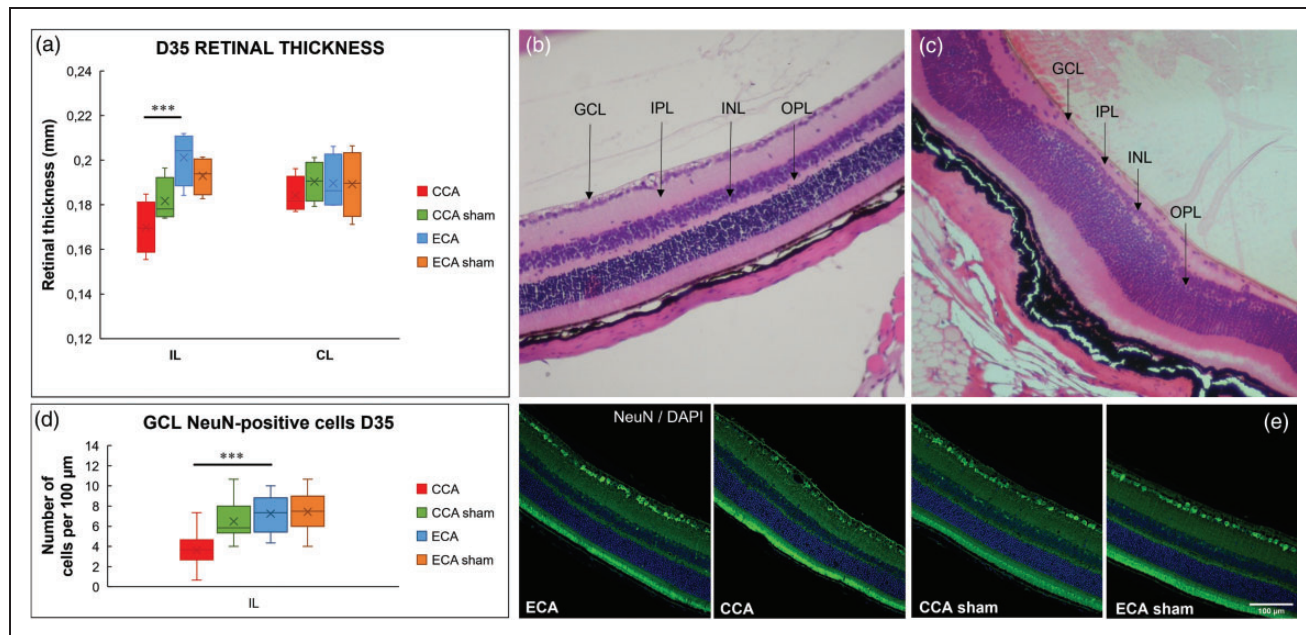


Figure 7. Histological and immunofluorescent staining reveals cell loss and thinning in the Koizumi (CCA) middle cerebral artery occlusion method. Average retinal thickness measured on the hemalaun/eosin-stained sections (a) 35 days after middle cerebral artery occlusion by filament insertion through the common carotid artery (CCA), the external carotid artery (ECA), and in sham-operated (CCA sham and ECA sham) animals, shows thinning of the ipsilateral (IL) retina in the CCA animals. Representative section of the contralateral (CL) retina of the CCA group 35 days after MCAO displays normal morphology (b). The IL retina in the CCA group (c) displays disrupted retinal morphology, a pronounced cell loss in the ganglion cell layer (GCL), thinning of the internal plexiform layer (IPL), cell loss in the internal nuclear layer (INL), and thinning of the outer plexiform layer (OPL). Immunofluorescent staining of retinal cross-sections 35 days after MCAO confirms NeuN-positive cell loss in the ganglion cell layer of the CCA IL retinas (d, e). Magnification 20 \times scale bar = 100 μ m. Statistical differences using mixed model ANOVA and Tukey post hoc test for the CCA to ECA group (***) $P < 0.001$. Data presented as median with interquartile range.

Histological and immunohistochemical analysis show alterations only in the CCA method

Histological and immunohistochemical analysis of the retinas 35 days after MCAO showed that prolonged hypoperfusion of the PPA and OA following a short 30-minute ischemia in CCA MCAO resulted in pronounced cell loss in the ganglion cell layer ($P = 0.0001$; Figure 7(c), (d) and (e)), thinning of the inner plexiform layer, cell loss in the inner nuclear layer, and thinning of the outer plexiform layer (Figure 7(c)). The IL retinas of the CCA-MCAO group displayed significant thinning compared to the ECA-MCAO group ($P = 0.0004$; Figure 7(a)). In the CCA-sham group, three of the eight IL retinas displayed thinning of the outer plexiform layer, while the other five showed no obvious morphological alterations. The IL and CL retinas of the ECA-MCAO and ECA-sham groups did not show changes in retinal morphology, as well as the CL retinas of the CCA groups (Figure 7(a) and (b)).

Discussion

To the best of our knowledge, this is the first report to examine and compare the long-term status of cerebral

and retinal vascular perfusion after the induction of acute ischemic brain injury using the Koizumi and Longa middle cerebral artery occlusion models, and the first to provide concurrent anatomical evidence of the origin of the ophthalmic artery in mice.

Only two other studies directly compared the Koizumi and Longa methods in mice, both assessing only the short-term effects of the two methods.^{31,32} Contrary to the study of Smith et al., showing higher mortality rate for the Koizumi method after 24 hours, we showed no difference between the methods in the acute phase and a 22% greater long-term survival following the Koizumi method. The premise that complete reperfusion after filament removal should occur in the ILH due to the nature of the Circle of Willis was shown to be incorrect by both our data and the aforementioned studies.^{31,32} The fact that reperfusion reached only 55% of baseline values in the Koizumi group, 72% in the Koizumi-sham group, and 100% in the Longa group, led us to further explore the duration of this hypoperfused state in the Koizumi method by MRA. The MIP analysis of MR angiograms revealed significant differences in the long-term perfusion status of the brain between the Longa and

Koizumi methods. Although laser-Doppler measurements showed full reperfusion after filament withdrawal in the Longa method, two days after MCAO the MIP revealed lower signal intensity of the MCA with a hypoperfused segment between IL ACA and MCA. Complete perfusion was reestablished after a week. In contrast, the hypoperfusion measured at the time of filament withdrawal in the Koizumi method was persisting in the subacute phase, not only in the MCA but in the entire ILH. Only after a week, partial reestablishment of perfusion in the Circle of Willis, PCA, proximal MCA, and ACA was shown. The measured arterial volume did not reach baseline values even 35 days after MCAO, suggesting that the Koizumi method should be considered a model of ischemia with chronic hypoperfusion rather than of ischemia and reperfusion, the latter being modeled by the Longa method. This was further supported by our analysis of the recruitment of IL PcomA as an arterial collateral, which is a compensatory phenomenon occurring secondary to hypoperfusion.^{28,29} Our analysis clearly demonstrated this phenomenon in the Koizumi group, but not in the Longa group. The most likely reason for the documented differences in reperfusion between the models is the permanent ligation of IL CCA in Koizumi vs transient ligation with full post-MCAO reperfusion of the IL CCA in Longa model, as previously suggested by others^{31,32} and confirmed in our angiograms. Thus, when translating to the clinical setting, we propose the Koizumi method as a model of spontaneous slow recanalization of the occluded artery and the Longa method as a model for fast recanalization as in the case of thrombolytic therapy or thrombectomy.

In contrast to both Smith's and Morris's studies, where no difference in lesion volume was found at 24 hours post-MCAO, we showed a noticeably larger lesion volume in the acute phase in the Longa group, suggesting that fast recanalization promotes edema formation, potentiating secondary damage. The discrepancy between the studies could be due to different time points (24 vs. 48 hours) or different assessment methods (MRI vs. TTC-staining). After the edema resolved, as indicated by the reduction in ILH swelling a week after MCAO, both Koizumi and Longa groups exhibited pronounced atrophy of the ILH, with significantly greater tissue loss in the Longa group. Fast recanalization in the Longa method promoted substantial edema formation and secondary damage, leading to greater tissue loss, as shown for thrombolysis in the clinic after the safe window of 4.5 hours of ischemia is surpassed.³³ However, more attention should be paid to the effects of hypoperfusion in the Koizumi group, which caused the development of smaller lesions in the acute phase of ischemia and led to less pronounced

atrophy in the chronic phase, suggesting a possible beneficial effect of hypoperfusion in the evolution of ischemic lesion.

The neurological status following MCAO corresponded to the lesion volume data only in the acute phase, showing significantly higher deficit for the Longa group compared to the Koizumi group, which is in accordance with the data from Smith et al.³¹ In the chronic phase, only differences in postural signs were observed between the MCAO groups, although the Longa group exhibited substantially greater tissue loss. Neither group fully recovered to its baseline levels. One of the limitations of our work was the measurement of a general neurological status, which covers a variety of functions that are rather unspecific and may fail to detect subtle chronic functional differences. To confirm our chronic data, a more specific and detailed behavioral characterization should be performed in the future.³⁴

There is a recurring erroneous premise in many pre-clinical studies, including even recent ones, that the occurrence of retinal ischemia after MCAO-induced ischemic stroke in these murine models is likely due to the proximity of the OA to the MCA.^{12,14,15,35} This presumption lacks any anatomical evidence in mice, and contradicts the existing anatomical knowledge of rat vasculature, misrepresenting the mechanism by which the co-occurring retinal ischemia develops, which has already been pointed out by others.²³ Using MR angiography, we established that in all our C57Bl/6J mice the PPA gave rise to the OA, further corroborating this with gross anatomical findings, and therefore confirming previous suggestions.^{23,24} By comparing the MIP of the longitudinally acquired MR angiograms, we showed that the perfusion status of the PPA and OA was solely affected when the Koizumi method was applied. Permanent ligation of the CCA in the Koizumi method induced permanent hypoperfusion to the ICA, affecting the PPA as its branch, in both Koizumi and sham-Koizumi surgeries. The Longa and Longa-sham groups showed no changes in the perfusion of the PPA or OA in the days after ischemia induction, suggesting immediate reperfusion of the blood flow to the retina after filament withdrawal.

Acute ischemia with chronic hypoperfusion following the Koizumi method induced a similar ischemic lesion evolution pattern as in the brain, with thickening of the retina in the acute phase followed by edema resolution and thinning of the retina in the chronic phase of ischemia. Moreover, we demonstrated histological evidence of permanent morphological changes following the Koizumi surgery, including cell loss in the ganglion cell layer and the inner nuclear layer, and thinning of the inner and outer plexiform layers,

which is in accordance with previous subacute studies using a similar surgery approach in rats.⁷ The immunohistochemical analysis further confirmed the histologically evident and extensive ganglion cell loss in the Koizumi method. In contrast to the Koizumi method, we did not observe any long-term changes in the retina in the Longa method in which 30 minutes of occlusion were followed by immediate reperfusion. Our findings are well corroborated by other acute and subacute studies, showing no apparent histological alterations when the Longa method was used.^{15,35,36} Obviously, the length of the occlusion plays a key role in the outcome. Since in our study (and in the Koizumi and Longa MCAO models in general) the site of the acute occlusion affecting the retina is at the origin of the PPA, the closest comparable model of retinal ischemia in itself is the model of temporary ligation of the PPA, described by Lelong et al.²³ In this model, which also included the ligation and section of the ECA, the 30-minute occlusion of the PPA, similarly as in our Longa group, produced no apparent histological changes 4 weeks after the ischemic event, but longer occlusion periods produced obvious atrophy of the inner retinal layers.^{23,24} The striking difference in retinal and cerebral response to the Longa method might lie in the fact that retina seems to show greater tolerance to ischemia.^{12,14,15,37–39} Due to a limitation in our methodology of retinal assessment (MRI), it is possible that by using other methods of assessment, such as electroretinography, fundus photography, or fluorescein angiography, we could detect more subtle changes in retinal responses after MCAO surgery.

In conclusion, using MRA to monitor the long-term status of cerebral vascular perfusion, we redefined the Koizumi method as a model of ischemia with chronic hypoperfusion, as opposed to the Longa method, which models ischemia and reperfusion; a distinction one should bear in mind when translating to clinical settings. This was the first MCAO study to provide anatomical evidence of the origin of the ophthalmic artery in mice, showing that it arises from the pterygopalatine artery, and the first to compare the co-occurring retinal ischemia in the two models, suggesting that most retinal responses to ischemia overlap with those in the brain when the Koizumi method is performed, with evident atrophy of the inner retinal layers in the wake of acute ischemia with hypoperfusion. In contrast, the Longa method, which resulted in a more extensive cerebral lesion with greater tissue loss compared to the Koizumi method, produced no apparent MR or histological lesions of the retina. Improvement in preclinical modeling of retinal ischemia co-occurring with stroke is necessary for a better understanding of the pathophysiological processes underlying cerebral and retinal ischemia.

Availability of data and materials

The data used and analyzed in the current study are available from the corresponding authors upon request.

Funding

The author(s) disclosed receipt of the following financial support for the research, authorship, and/or publication of this article: This work was funded by the Croatian Science Foundation project BRADISCHEMIA (UIP-2017-05-8082) and Scientific Centre of Excellence for Basic, Clinical and Translational Neuroscience project “Experimental and clinical research of hypoxic-ischemic damage in perinatal and adult brain”; GA KK01.1.1.01.0007 funded by the European Union through the European Regional Development Fund. The work of doctoral students Anja Barić and Rok Ister has been fully supported by the “Young researchers’ career development project – training of doctoral students” of the Croatian Science Foundation funded by the European Union from the European Social Fund.

Declaration of conflicting interests

The author(s) declared no potential conflicts of interest with respect to the research, authorship, and/or publication of this article.

Authors’ contributions

H.J. performed MR data analysis, histology and immunohistochemistry with image analysis, wrote the manuscript; A.B. performed MR imaging, neurological scoring and analysis, wrote the manuscript; I.Š. script design for image postprocessing and MRA analysis; S.Š. script design for image postprocessing, designed and performed MR imaging; M.R. designed research, contributed to the writing and editing of the manuscript; R.I. performed PcomA recruitment analysis; M.D.R. designed research, performed MCAO, statistical analysis, revised the manuscript. All authors contributed to revising of the manuscript.

ORCID iDs

Iva Šimunić  <https://orcid.org/0000-0002-4411-0194>
Marin Radmilović  <https://orcid.org/0000-0003-2847-0525>
Siniša Škokić  <https://orcid.org/0000-0002-9065-9129>
Marina Dobrivojević Radmilović  <https://orcid.org/0000-0002-2513-1889>

Supplemental material

Supplemental material for this article is available online.

References

1. Hepworth L, Rowe F, Walker M, et al. Post-stroke visual impairment: a systematic literature review of types and recovery of visual conditions. *Ophthalmol Res* 2016; 5: 1–43. doi:10.9734/or/2016/21767.
2. Rowe FJ. Stroke survivors’ views and experiences on impact of visual impairment. *Brain Behav* 2017; 7: e00778. doi:10.1002/brb3.778.

3. Chodnicki KD, Pulido JS, Hodge DO, et al. Stroke risk before and after central retinal artery occlusion in a US cohort. *Mayo Clin Proc* 2019; 94: 236–241. doi:10.1016/j.mayocp.2018.10.018
4. Scoles D, McGeehan B and VanderBeek BL. The association of stroke with central and branch retinal arterial occlusion. *Eye (Lond)* 2022; 36: 835–843. doi:10.1038/s41433-021-01546-6.
5. Kim YD, Kim JY, Park YJ, et al. Cerebral magnetic resonance imaging of coincidental infarction and small vessel disease in retinal artery occlusion. *Sci Rep* 2021; 11: 864. doi:10.1038/s41598-020-80014-9.
6. Vestergaard N, Torp-Pedersen C, Vorum H, et al. Risk of stroke, myocardial infarction, and death among patients with retinal artery occlusion and the effect of antithrombotic treatment. *Transl Vis Sci Technol* 2021; 10: 2. doi:10.1167/tvst.10.11.2.
7. Kingsbury C, Heyck M, Bonsack B, et al. Stroke gets in your eyes: stroke-induced retinal ischemia and the potential of stem cell therapy. *Neural Regen Res* 2020; 15: 1014–1018. doi:10.4103/1673-5374.270293.
8. Liu F and McCullough LD. Middle cerebral artery occlusion model in rodents: methods and potential pitfalls. *J Biomed Biotechnol* 2011; 2011: 464701–464709. doi:10.1155/2011/464701.
9. Koizumi J, Yoshida Y, Nakazawa T, et al. Experimental studies of ischemic brain edema. *Jpn J Stroke* 1986; 8: 1–8.
10. Longa EZ, Weinstein PR, Carlson S, et al. Reversible middle cerebral artery occlusion without craniectomy in rats. *Stroke* 1989; 20: 84–91. doi:10.1161/01.str.20.1.84.
11. Block F, Grommes C, Kosinski C, et al. Retinal ischemia induced by the intraluminal suture method in rats. *Neurosci Lett* 1997; 232: 45–48. doi:10.1016/S0304-3940(97)00575-2.
12. Steele EC, Guo Q and Namura S. Filamentous middle cerebral artery occlusion causes ischemic damage to the retina in mice. *Stroke* 2008; 39: 2099–2104. doi:10.1161/STROKEAHA.107.504357.
13. Kalesnykas G, Tuulos T, Uusitalo H, et al. Neurodegeneration and cellular stress in the retina and optic nerve in rat cerebral ischemia and hypoperfusion models. *Neuroscience* 2008; 155: 937–947. doi:10.1016/j.neuroscience.2008.06.038.
14. Allen RS, Sayeed I, Cale HA, et al. Severity of middle cerebral artery occlusion determines retinal deficits in rats. *Exp Neurol* 2014; 254: 206–215. doi:10.1016/j.expneurol.2014.02.005.
15. Nguyen H, Lee JY, Sanberg PR, et al. Eye opener in stroke. *Stroke*. *Stroke* 2019; 50: 2197–2206. doi:10.1161/STROKEAHA.119.025249.
16. Marmor MF and Dalal R. Irregular retinal and RPE damage after pressure-induced ischemia in the rabbit. *Investig Ophthalmol Vis Sci* 1993; 34: 2570–2575.
17. Stevens WD, Fortin T and Pappas BA. Retinal and optic nerve degeneration after chronic carotid ligation. *Stroke* 2002; 33: 1107–1112. doi:10.1161/01.str.0000014204.05597.0c.
18. Lavinsky D, Arterni NS, Achaval M, et al. Chronic bilateral common carotid artery occlusion: a model for ocular ischemic syndrome in the rat. *Graefes Arch Clin Exp Ophthalmol* 2006; 244: 199–204. doi:10.1007/s00417-005-0006-7.
19. Huang Y, Fan S, Li J, et al. Bilateral common carotid artery occlusion in the rat as a model of retinal ischaemia. *Neuroophthalmology* 2014; 38: 180–188. doi:10.3109/01658107.2014.908928.
20. Leahy S, Farzad S, Blair NP, et al. Retinal oxygen delivery, metabolism, and extraction fraction during long-term bilateral common carotid artery occlusion in rats. *Sci Rep* 2020; 10: 10371. doi:10.1038/s41598-020-67255-4.
21. Fujii M, Hara H, Meng W, et al. Strain-related differences in susceptibility to transient forebrain ischemia in SV-129 and C57Black/6 mice. *Stroke* 1997; 28: 1805–1811. doi:10.1161/01.str.28.9.1805.
22. Eunice Chace Greene. *Anatomy of the rat*. New York: Hafner Publishing Company, 1963.
23. Lelong DC, Bieche I, Perez E, et al. Novel mouse model of monocular amaurosis fugax. *Stroke* 2007; 38: 3237–3244. doi:10.1161/STROKEAHA.107.499319.
24. Ogishima H, Nakamura S, Nakanishi T, et al. Ligation of the pterygopalatine and external carotid arteries induces ischemic damage in the murine retina. *Invest Ophthalmol Vis Sci* 2011; 52: 9710–9720. doi:10.1167/iovs.11-8160.
25. Erdfelder E, Faul F, Buchner A, et al. Statistical power analyses using G*power 3.1: tests for correlation and regression analyses. *Behav Res Methods* 2009; 41: 1149–1160. doi:10.3758/BRM.41.4.1149.
26. Garcia JH, Wagner S, Liu K-F, et al. Neurological deficit and extent of neuronal necrosis attributable to middle cerebral artery occlusion in rats. *Stroke* 1995; 26: 627–635. doi:10.1161/01.str.26.4.627.
27. Li Y, Chopp M, Chen J, et al. Intraatrial transplantation of bone marrow nonhematopoietic cells improves functional recovery after stroke in adult mice. *J Cereb Blood Flow Metab* 2000; 20: 1311–1319. doi:10.1097/00004647-200009000-00006.
28. Knauss S, Albrecht C, Dirnagl U, et al. A semiquantitative non-invasive measurement of PcomA patency in C57BL/6 mice explains variance in ischemic brain damage in filament MCAo. *Front Neurosci* 2020; 14: 576741. doi:10.3389/fnins.2020.576741.
29. Foddis M, Winek K, Bentele K, et al. An exploratory investigation of brain collateral circulation plasticity after cerebral ischemia in two experimental C57BL/6 mouse models. *J Cereb Blood Flow Metab* 2020; 40: 276–287. doi:10.1177/0271678X19827251.
30. Wang T, He M and Zha X. Time-dependent progression of hemorrhagic transformation after transient ischemia and its association with GPR68-dependent protection. *Brain Hemorrhages* 2020; 1: 185–191. doi:10.1016/j.hest.2020.10.001.

31. Smith HK, Russell JM, Granger DN, et al. Critical differences between two classical surgical approaches for middle cerebral artery occlusion-induced stroke in mice. *J Neurosci Methods* 2015; 249: 99–105. doi:10.1016/j.jneumeth.2015.04.008.
32. Morris GP, Wright AL, Tan RP, et al. A comparative study of variables influencing ischemic injury in the Longa and Koizumi methods of intraluminal filament middle cerebral artery occlusion in mice. *PLoS One* 2016; 11: e0148503. doi:10.1371/journal.pone.0148503.
33. Baron JC. Selection of patients for thrombectomy in the extended time window. *JAMA Neurol* 2021; 78: 1051–1053. doi:10.1001/jamaneurol.2021.1825.
34. Balkaya M, Kröber JM, Rex A, et al. Assessing post-stroke behavior in mouse models of focal ischemia. *J Cereb Blood Flow Metab* 2013; 33: 330–338. doi:10.1038/jcbfm.2012.185.
35. Lee J, Castelli V, Bonsack B, et al. Eyeballing stroke: blood flow alterations in the eye and visual impairments following transient middle cerebral artery occlusion in adult rats. *Cell Transplant* 2020; 29: 963689720905805. doi:10.1177/0963689720905805.
36. Ritzel RM, Pan SJ, Verma R, et al. Early retinal inflammatory biomarkers in the middle cerebral artery occlusion model of ischemic stroke. *Mol Vis* 2016; 22: 575–588.
37. Lee JM, Grabb MC, Zipfel GJ, et al. Brain tissue responses to ischemia. *J Clin Invest* 2000; 106: 723–731. doi:10.1172/JCI11003.
38. Hayreh SS, Zimmerman MB, Kimura A, et al. Central retinal artery occlusion. Retinal survival time. *Exp Eye Res* 2004; 78: 723–736. doi:10.1016/s0014-4835(03)00214-8.
39. Hayreh SS and Jonas JB. Optic disk and retinal nerve fiber layer damage after transient Central retinal artery occlusion: an experimental study in rhesus monkeys. *Am J Ophthalmol* 2000; 129: 786–795. doi:10.1016/s0002-9394(00)00384-6.